Venus: The corona co

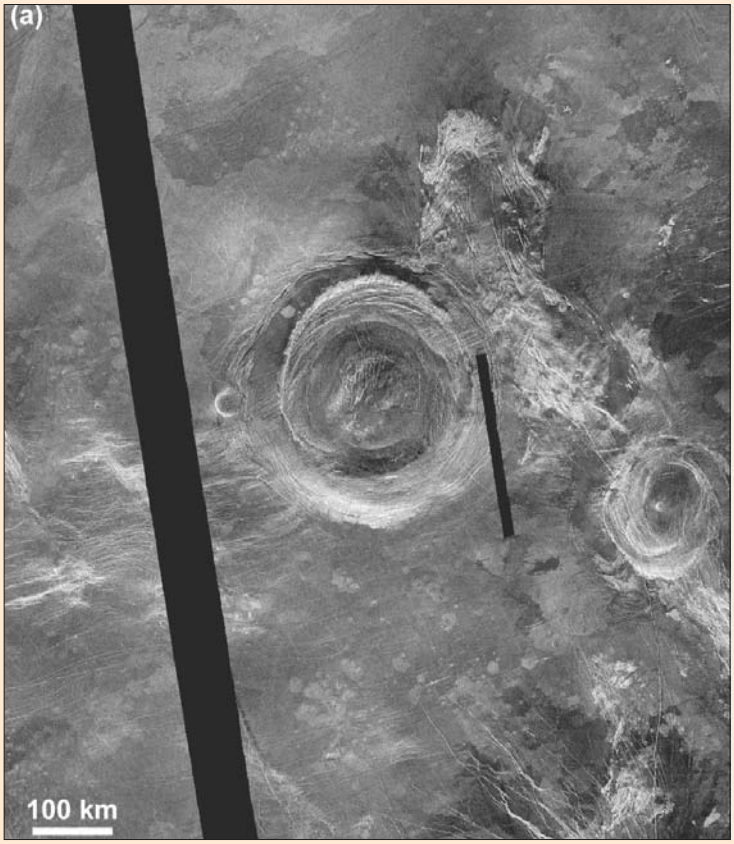

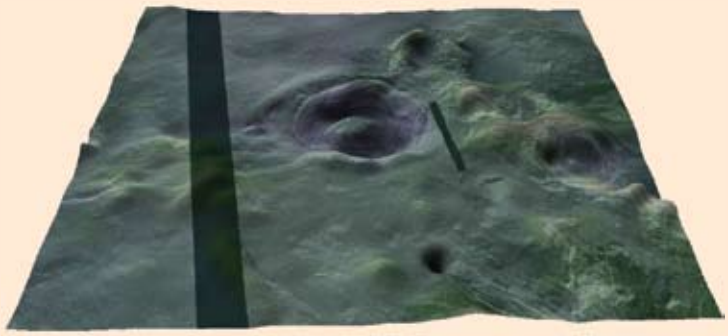

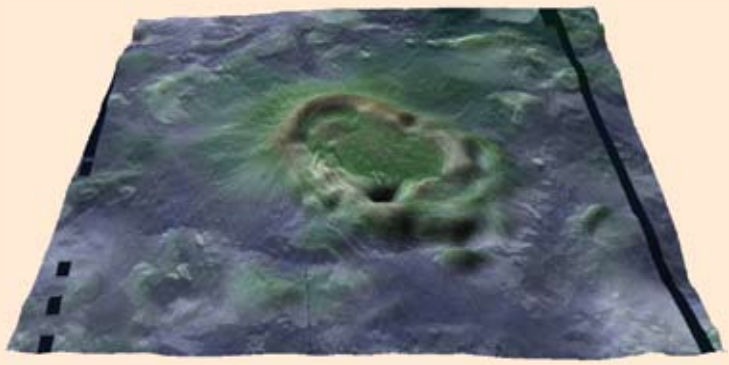

(a) Aramaiti Corona (25.5°S, 82.0°E), a concentric corona ~350 km in diameter which displays a well-defined annulus of concentric fractures. Note the small-scale volcanism in the centre and larger-scale volcanism where radar-dark material has flooded the topographic moat.

(b) Aruru Corona (9.0°N, 262.0°E), has a diameter of ~450 km and shows evidence of extensive interior and exterior volcanism.

ABSTRACT

Coronae are large circular features on Venus, whose complex structure, with traces of tectonic and volcanic activity, mean that their origin remains enigmatic. Their non-random distribution, complex geological histories and associated volcanic features have been explained most successfully by models involving mantle upwelling. In this paper, we summarize the models of their formation to date, paying particular attention to the success, as well as shortcomings, of these mantle upwelling models. We also describe recent models and theories which have highlighted the need for further investigation into the origin of coronae, with the aim of better understanding the evolution of the interior and surface of Venus.

Investigation of the coronae on Venus began when large circular structures of unknown origin were identified in radar data from Goldstone (Schaber and Boyce 1977) and Arecibo (Campbell and Burns 1980). Soon afterwards similar features were found with Pioneer Venus images and altimetry (Masursky *et al.* 1980). But it was with the first Synthetic Aperture Radar (SAR) data returned from Veneras 15 and 16 in the early 1980s that interest dramatically increased in these strange features. Barsukov *et al.*(1984) presented an initial general

nundrum

Peter M Grindrod and Trudi Hoogenboom revisit the odd annular structures so characteristic of the surface of Venus.

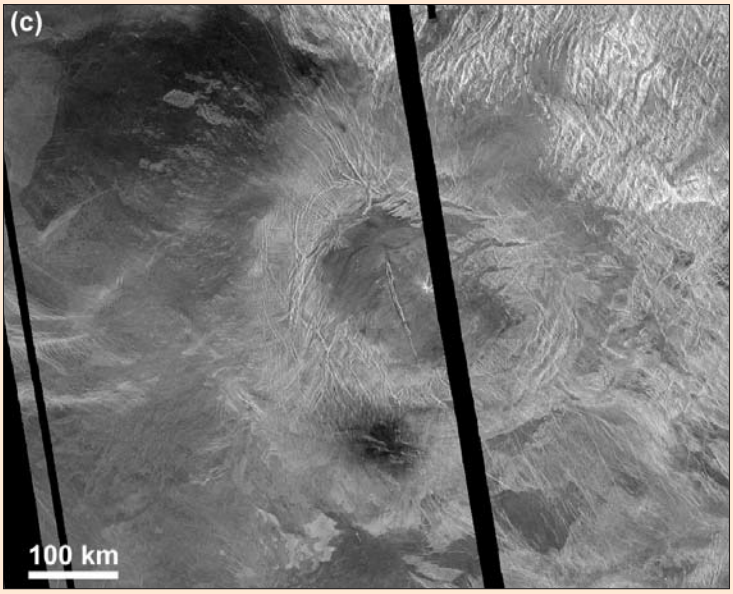

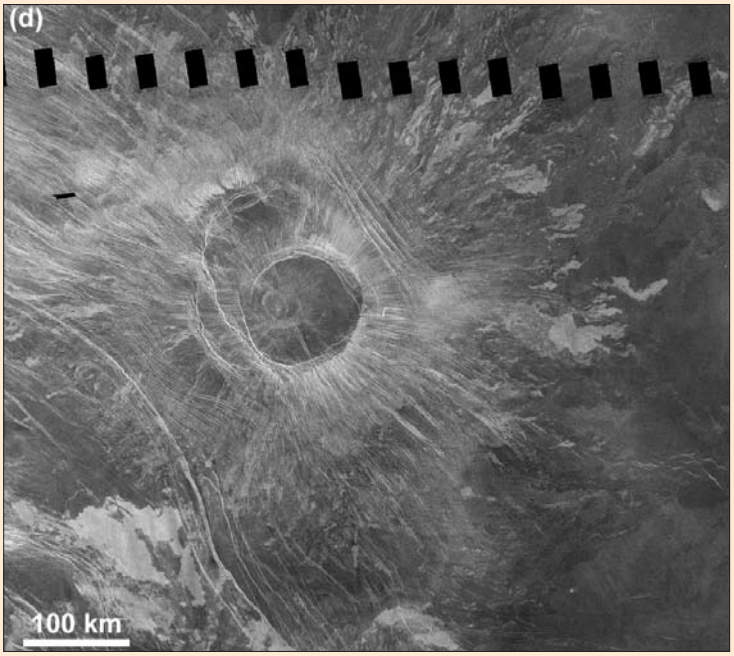

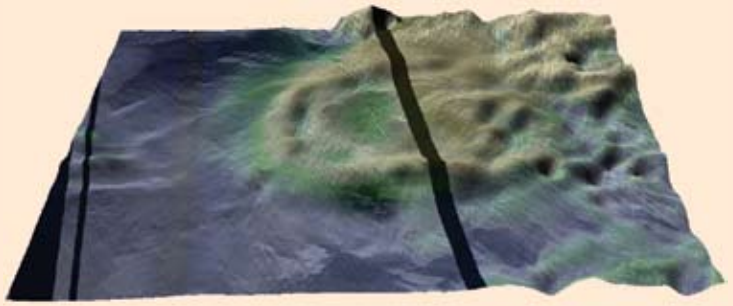

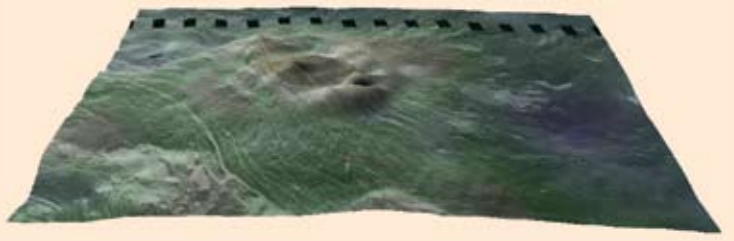

(c) Eve Corona (32.0°S, 259.8°E), has a diameter of ~330 km and is situated on the edge of some tessera terrain. Note the radial and concentric fracturing, in addition to the radial lava flows north-west and west.

(d) Nagavonyi Corona (18.5°S, 259.0°E), has a diameter of ~190 km, has two main sets of concentric fractures in addition to extensive rift-related fractures. Note the almost complete radial lava flow apron, with flows extending up to 200 km from the topographic rim.

1: Upper images: Magellan left-looking Synthetic Image Radar (SAR) images of some coronae on Venus, all in Mercator projection. Black lines are regions of missing Magellan SAR data. Lower images: 3-D perspective images of the same coronae, created by combining the Magellan altimetry data with SAR images. Vertical exaggeration is ~10 times in each image. Colours correspond to relative height, with blues and greens corresponding to low elevation regions and yellows and whites to higher regions. Note the shape and relative height of the topographic rim in each case.

description of complex circular to oval structures surrounded by an annulus consisting of multiple concentric ridges. In 1986 Barsukov *et al.* (1986) christened these features "coronae", derived from the Latin term for crown.

Coronae are thought to be unique to Venus, although they are similar to features on Earth (Herrick 1999, Lopez *et al.* 1999), Mars (Watters and Janes 1995) and Miranda (Anguita and Chiccaro 1991). They range in diameter from 75 to over 1000 km across (Stofan *et al.* 1992), are distributed across Venus in various geologic settings (Stofan *et al.* 1997) and appear in complex volcanic, tectonic and topographic variations (Squyres *et al.* 1992, Stofan *et al.* 1992, 1997). Figure 1 show s the variety of forms; the box on pages 3.xx summarizes their observed characteristics. The coronae represent a crucial part of the geodynamic evolution of the venusian surface and may also contribute to the release of heat from the interior of the planet (Smrekar and Stofan 1997). But how did they form? This has been the most intriguing question since their discovery and remains contentious.

Corona formation mechanisms

The first hypotheses for the formation of coronae based on Venera data (Barsukov *et al.* 1984) centred on ideas of upwelling and related volcanism. These were followed by many more as NASA's Magellan orbiter used radar to map Venus in much greater detail. These included: impact crater rejuvenation (Nikolaeva *et al.* 1986); ring-dike intrusion (Masursky 1987); lithospheric subduction (Sandwell and Schubert 1992, McKenzie *et al.* 1992b); sinking and/or rising mantle diapirs (Stofan *et al.* 1987); gravitational relaxation

Observations of coronae

The many coronae on the surface of Venus – 513 in all (Stofan *et al.* 2001) – together with their potential for understanding mantle processes, has resulted in intense study of their characteristics. Before the Magellan mission (1990–1994), only 36 corona and similar features had been identified in Venera 15/16 data (Pronin and Stofan 1990). These data showed that coronae appeared to form preferentially in clusters. The global data set of Magellan increased the number of coronae observations to approximately 360 and showed that although they occur over most of the planet's surface, their distribution is non-random (Stofan *et al.* 1992, Squyres *et al.* 1993). Further analysis using Magellan synthetic stereo images increased the number of coronae observed to the current value of 513.

Coronae are found in three distinct geological environments: on topographic rises, as relatively isolated features in the plains (25%), and along chasmata (62%). There are exceptions, including three coronae located on Lakshmi Planum (a volcanic highland plateau) and five in tessera terrain (Glaze *et al.* 2002). Coronae located on topographic rises are larger than coronae found elsewhere (Glaze *et al.* 2002). Plains coronae are often embayed by plains volcanism, and include some of the largest coronae (Stofan *et al.* 1997).

The majority of coronae are clustered along chasmata or fracture belts in the Beta-Atla-Themis zone (figure 1). Chasmata coronae occur in chains roughly aligned with the fracture belt (Stofan *et al.* 1997). There is no evidence for a systematic age progression among coronae in chains at the major rift zones Hecate (Hamilton and Stofan 1996) and Parga (Martin and Stofan 2004) Chasmata. In addition, there are no clear trends in relative timing between coronae and rift formation at chasmata, indicating that the processes that influence their formation may operate to varying degrees at different locations (Hamilton and Stofan 1996, Martin and Stofan 2004).

The hypsometric distribution of coronae has also been investigated. There are more coronae in the elevation range of 6051.5 and 6052.5 km than would be expected from a random distribution (Squyres *et al.* 1993), suggesting that coronae are concentrated in a narrow elevation band close to the mean geoid value, avoiding the lowest and highest elevations (Squyres *et al.* 1993).

Tectonism

The style of tectonic deformation observed at coronae is distinctive enough to be the primary method of recognition. Most coronae have a ring of closely spaced concentric fractures and/or ridges, superimposed on a raised rim, as shown in figure 1 (Stofan *et al.* 2001). The annulus width varies from 10 to over 150 km, but tends to be less than half of the radius of the coronae (Stofan *et al.* 1992). The annulus is dominated by extensional graben and other fractures, but there are also often compressional ridges (Stofan *et al.* 1997). Lava flows that originate from the corona interior, or even the annulus itself, often embay and obscure corona annuli (Stofan *et al.* 1997). The complicated histories at coronae revealed by photogeological mapping demonstrated that the formation of corona annuli can be multi-staged, and that the position of the annuli does not always coincide with the topography at the feature (Copp *et al.* 1998).

The discovery of so-called "stealth" coronae, of topography (Stofan *et al.* 1987, Stofan *et al.* 1991); and hot-spot or rising diapiric intrusions (Basilevsky *et al.* 1986, Stofan *et al.* 1987). Each of these mechanisms, and its relation to characteristics of the coronae, is described below.

Impact craters

Nikolaeva *et al.*(1986) suggested that the coronae were impact craters modified by volcanism and tectonic activity, a mechanism previously suggested for features on the Moon and Mars (Schultz 1976, Schultz and Glicken 1979). Lithosphere weakened by an impact acts as a source for lava flows that bury the crater. This model predicts transitional features between pristine and rejuvenated impact craters that have not been found on Venus. The model also fails to account for the raised topography or complex tectonism associated with coronae (Stofan and Head 1990). In addition, most venusian craters are a lot smaller than most coronae (Herrick *et al.* 1997), suggesting distinct origins.

There have been attempts recently to revive the impact theory. Vita-Finzi *et al.*(2005) suggest that many coronae are old, degraded impact craters, noting that the combined crater and corona population fit a log-normal frequency distribution, similar to the crater population of other terrestrial bodies. Hamilton (2005) questions the transfer of terrestrial plume theory to Venus, thus favouring an ancient impact origin. If impacts are indeed responsible for coronae, the implications are significant: the surface of Venus could be significantly older than thought and dominated by sediments, rather than volcanism. However, this origin is still not in favour, because it cannot account for the clustering of coronae in rift zones, which are likely to be some of the youngest areas on Venus (Price *et al.* 1996), nor does it account for the complexities seen at individual coronae (e.g. Copp *et al.* 1998).

Ring-dike intrusion

On Earth, ring-dike complexes can be surrounded by ridges of similar morphology to those observed at coronae, and Masursky (1987) suggested that coronae may have formed in a similar way. Terrestrial ring-dike complexes form as a result of multiple igneous intrusions around a central stock, showing as concentric patterns at the surface (Anderson 1924). But the morphology seen on Earth results from relatively fast differential erosion, and erosion on Venus is too slow and would produce different results (Arvidson *et al.* 1992, Stofan and Head 1990). Ring-dyke complexes also do not feature the outer topographic low shown by many coronae (Stofan and Head 1990). In addition, coronae can be as much as 50 times larger than these terrestrial features.

Lithospheric subduction

With the initial results from Magellan, McKenzie *et al.* (1992b) compared the curvature and topography at trenches on Venus to those at terrestrial subduction zones. They argued that many venusian trenches exhibited similar patterns of curvature and topographic asymmetry and therefore might result from lithospheric subduction. This theory was extended to coronae by Sandwell and Schubert (1992), who suggested that retrograde lithospheric subduction occurs on the outside margins of large coronae (such as Artemis Chasma), with compensating back-arc extension in the interior. This was supported by a gravity study of four coronae whose apparent depths of compensation were consistent with subduction or underthrusting (Schubert *et al.* 1993). However, subsequent detailed mapping studies have found inconsistencies (e.g. Hansen and Phillips 1993). For example, many coronae exhibit continuous radial fractures stretching beyond the edge of the corona rim or trough (Hamilton and Stofan 1996). If the fractures resulted from subduction, they should not continue beyond the trench; if they formed before subduction, they might be expected to display significant offset or difference in orientation on either side of the trench (Hansen and Phillips 1995). In addition, many smaller coronae do not display evidence of extension in their interiors, which should be a clear consequence of retrograde subduction on the perimeter (Hamilton and Stofan 1996).

Mantle upwelling

Observations of elevated topography, volcanism, circular shape and extensional tectonism, led investigators to suggest upwelling, specifically from the mantle, as a mechanism for corona formation (Barsukov *et al.* 1984, 1986, Basilevsky *et al.* 1986, Stofan *et al.* 1992). The high surface temperature on Venus led to the supposition that materials at shallow depths would exhibit ductile

identifiable only in topographic and synthetic stereo images (Tapper 1997), led to the definition of a corona being modified to cover two distinct types. Type 1 coronae are surrounded by an annulus of >180° of arc (50% of circumference), and make up most of the population. Type 2 coronae have less than 180° arc of fracturing and often have no concentric fracturing at all, but do usually have a well-defined topographic rim (Stofan *et al.* 2001). Statistical analysis has shown that most Type 1 coronae are located along chasmata systems or fracture belts, while Type 2 coronae tend to be isolated features in the plains (Glaze *et al.* 2002).

In addition to concentric fractures, coronae often show other signs of tectonic deformation. Radial fractures, usually originating from the centre of the corona, are common (Aittola and Kostama 2002) and often extend for lengths much greater than the corona radius (McKenzie *et al.* 1992a, Grosfils and Head 1994). Many radial fractures appear to predate concentric fractures (Stofan *et al.* 1997), although there are several exceptions to this rule (Aittola 2001).

Topographic profile

Coronae display a wide range of topographic profiles (table 1) which have been classified into nine groups (Smrekar and Stofan 1997): (1) dome, (2) plateau, (3a) rim surrounding interior high, (3b) rim surrounding interior dome, (4) rim surrounding interior depression, (5) outer rise, trough, rim, inner high, (6) outer rise, trough, rim, inner low, (7) rim only, (8) depression, and (9) no discernible signature. Examples of coronae topographic profiles are also shown in figure 1.

The most common Type 1 corona is group 4 while Type 2 coronae are most often in group 7 (Glaze *et al.* 2002). When viewed as a single population, group 4 coronae are the most common, accounting for ~26% of the total. Coronae with domes, depressions and rimmed depressions have smaller diameters than the other topographic profiles (Glaze *et al.* 2002).

Corona topography varies between 0.6 km below, and 4.5 km above the local elevation level, with a mean value of about 0.9 km higher, thus the majority of coronae are topographically raised (Glaze *et al.* 2002). The annulus corresponds with raised topography at most coronae (Stofan *et al.* 1997).

Volcanism

Many coronae have been affected by volcanism, ranging from small-scale vents to large, regional lava flow fields. Volcanic features in the interiors include vents, collapse pits and linear troughs, sinuous rilles, calderas, small (<20 km diameter) and intermediate (20–100 km) volcanoes, radar-bright and dark flows, and smooth plains deposits (Stofan *et al.* 1992). Some coronae resemble large (>100 km diameter) volcanoes, many of which are characterized by radial fractures and flows, which often bury concentric fractures (Grindrod *et al.* 2005, Herrick *et al.* 2005). Smooth plains deposits and domes are the most common volcanic features associated with the interiors (Stofan *et al.* 1992). The annulus itself often contains many smaller volcanic features, such as domes, cones and shields (Stofan *et al.* 1997). Exterior volcanic features include digitate and/or sheet flows, which vary in radar-brightness and can extend for large distances (Grindrod *et al.* 2005).

flow (Weertman 1978, Solomon *et al.* 1982). This principle implied that high topography, formed by uplift and/or volcanic loading, could relax relatively rapidly, and the stresses involved would form the observed ring of fractures around coronae (Stofan *et al.* 1987). It was then suggested that this process could modify topography raised as a result of diapiric uplift (Stofan and Head 1990, Stofan *et al.* 1991, Janes *et al.* 1992).

Stofan and Head (1990) suggested a three-stage scenario of coronae formation: (1) a hot source at depth causes uplift and volcanism at the surface, (2) continued volcanism, and gravitational relaxation of the high topography forms the annulus, and (3) the source at depth ceases, leaving gravitational relaxation as the dominant process. Although this viscoelastic relaxation model was able to produce an acceptable corona profile of a rim with an interior high and outer low, it couldn't account for the concentric fractures observed at many coronae (Janes and Squyres 1995).

Sinking diapir

In contrast to suggestions of corona formation via mantle upwelling, Stofan *et al.* (1987) also suggested a sinking diapir model of coronae formation. In this model, a phase change or cooling creates dense material at the base of the lithosphere. This material could be denser than the asthenosphere below, and so would begin to sink in isolated blobs as a Rayleigh–Taylor instability develops, like the descending blobs in a lava lamp. This would result in a topographic low over the surface around which the annular trough would develop. Compressional strain over the sinking diapir and more extensional strain near the periphery are predicted in this model (Stofan *et al.* 1991). However, neither dominant central compression nor depressions of the expected size have been observed, leading Stofan *et al.* (1991) to favour the upwelling mantle diapir model.

Numerical models of corona formation

As a result of the early successes in explaining corona topography and volcanism, numerical models of corona formation have predominantly addressed ascending, buoyant mantle plumes or diapiric upwellings (e.g. Stofan *et al.* 1991, Janes *et al.* 1992, Koch 1994, Koch and Manga 1996). Gravity and topography are the primary data sources for testing our understanding of mantle processes in Venus. As such, Magellan gravity and topography data have been used to test and validate numerical models of coronae formation.

The three-stage evolutionary model suggested by Stofan and Head (1990) was further developed by numerical models (Janes *et al.* 1991, Stofan *et al.* 1991). The first stage is uplift and/or construction forming a raised topographic feature, interior radial fracturing and volcanism. This is followed by the formation of a plateau and exterior volcanism. The final stage involves continued volcanism, formation of a central depression, topographic rim, and outer moat, and exterior concentric fracturing, a sequence that fits many coronae. But it does not fit all of them: some have never undergone an uplift phase (Stofan *et al.* 1997) or have multiple episodes of concentric fracture formation (Copp *et al.* 1998). To date, no completely self-consistent model of this entire evolutionary sequence has been developed (Stofan *et al.* 1997), although models have been developed for all stages in the sequence.

Stofan *et al.* (1991) employed a layered viscous model (Bindschadler and Parmentier 1990) to investigate the rise of a diapir through the mantle and the resulting surface uplift and stress. Viscosities in the crust and mantle layers were treated in a linear fashion, based on experimentally derived flow laws for diabase and olivine. The rising diapir was treated as an axisymmetric density anomaly at depth. Dome-shaped uplift at the surface is predicted, becoming taller and narrower as the diapir rises. [does this fit observations? --it sounds odd]

Janes *et al.* (1992) and Janes and Squyres (1993) employed a finite-element model which treated the rheological lithosphere as an elastic spherical shell with basaltic properties over a constant viscosity mantle (Janes and Melosh 1988). Although Janes and Squyres (1993) used non-Newtonian flow laws for the viscous constitutive relation of the asthenosphere, they linearized these laws by assuming that a constant characteristic stress operates throughout the relaxation process, thus effectively treating the viscosity as Newtonian. The diapir was modelled as a spherical region of buoyant mass at depth. Predicted domical uplift at the surface matches observed profiles of dome-shaped coronae. However, fits to topographic profiles using these

methodologies are non-unique because models have more free parameters (e.g. lithospheric/crustal thickness, diapir size, depth, density) than observational constraints (e.g. height, width of topography, diameter) (Stofan *et al.* 1997).

Gravitational relaxation of an isostatically uncompensated plateau was suggested for many of the early numerical models of corona formation (Stofan *et al.* 1991, Janes *et al.* 1992), and could produce the remaining observed corona topographic profiles. When an initially hot diapir cools, thermal buoyancy of the diapir should diminish and the upraised topography is then subject to gravitational relaxation (Stofan *et al.* 1997). This process was modelled by Stofan *et al.* (1991) who found that gravitational relaxation of an uncompensated plateau will produce a plateau shaped feature with a central depression (group 3a, table 1).

Janes and Squyres (1995) employed a viscous-elastic finite-element model with a layered power-law viscosity and a plastic failure envelope to determine the dominant response (elastic or viscous). In agreement with Stofan *et al.* (1991) they found that the model must start with a plateau in order for a rim and trough to form. By incorporating a dry diabase flow law (Mackwell and Kohlstedt 1993), they showed that the topography of the corona can persist over geological timescales, supported by the flexure of the lithosphere and isostatic buoyancy (Stofan *et al.* 1997).

Table 1: Topographic profiles of coronae

Group	Topographic profile	Description	%
1		Dome	10
2		Plateau	10
3a		Rim surrounding interior high	8
3b		Rim surrounding interior dome	13
4		Rim surrounding depression	25
5		Outer rise, trough, rim, inner high	5
6		Outer rise, trough, rim, inner low	1
7		Rim only	7
8		Depression	7
9		No discernible signature	14

Classification and percentage of coronae on Venus according to topographic shape. Vertical tick marks on topographic profiles indicate the typical location of fracture annuli, if present, for each group. (Table adapted from Smrekar and Stofan [1997])

Diapir geometry

The models discussed above predominantly assume spherical diapirs. But 10% of all coronae are plateau-shaped (Stofan *et al.* 2001), implying that any diapir responsible for producing this topography has begun to flatten out against the base of the lithosphere (Stofan *et al.* 1997). Koch (1994) modelled the rise and deformation of a buoyant, initially spherical, diapir through a constant viscosity mantle. A free-slip upper boundary condition was applied to the upper surface. Contrary to most plume models of corona formation, the model includes arbitrary viscosity and density contrast between the diapir and the surrounding fluid. As the diapir rises it produces a broad plateau at the surface, with a radius comparable to that of the flattened diapir.

The model described by Koch (1994) explicitly neglects the thermal effects that drive the diapir motion. Musser and Squyres (1997) employed a finite-element model that solved the coupled equations of viscous flow and heat conduction to investigate the rise and flattening of an originally spherical diapir. In addition, they investigated the effect of temperature and stress-dependent viscosity. Despite the added model complexities, these models were unable to predict the depressions observed at coronae.

The models described above predict only domes (e.g. Stofan *et al.* 1991, Janes *et al.* 1992, Musser and Squyres 1997) or require topographic relaxation of an initially steep-sided plateau to produce coronae with depressed interiors (Stofan *et al.* 1991, Janes and Squyres 1995). Koch and Manga (1996) demonstrated that coronae with raised rims and interior depressions could be modelled by an initially spherical diapir that spreads laterally at a depth of neutral buoyancy (called the spreading-drop model). They studied a diapir with uniform density and viscosity rising through a two-layer medium, where each layer has uniform viscosity, and solved for topography on the upper free-slip surface by using a boundary integral method. The level of neutral buoyancy may lie within the lithosphere, between the mantle and the crust (Hansen and Phillips 1993) or along a possible gabbro-eclogite phase transition (Koch and Manga 1996).

Viscosity

While mantle rocks such as olivine have a viscosity that varies strongly with temperature and depth, the majority of the models described above assume simplified thermal and viscosity structure of the mantle and lithosphere (e.g. Janes *et al.* 1992, Janes and Squyres 1993, Koch and Manga 1996). Smrekar and Stofan (1997), however, developed a 2-D axisymmetric finite-element model of corona formation in which the mantle is represented as a Newtonian temperature-dependent viscous fluid, with constitutive relation based on standard rheological models. In this model, a thermal plume of finite duration rises and interacts with the surface. Downwelling occurs at the edge of the spreading plume, removing or delaminating the lower lithosphere. By including the deformation of a pre-existing (low-density) layer of depleted mantle beneath the lithosphere (by the upwelling and delaminating lithosphere), the entire range of topographic forms can be predicted. The diverse topographic forms arise in different stages of evolution of this system, allowing for variation in model parameters. The presence of the low-density layer is necessary to produce rim-only coronae. In their calculations, topographic rims were produced by resistance to delamination at depth (where a central high or low is also present) or by isostatic re-adjustment of the depleted (low-density) mantle layer following thermal equilibration of the delaminated lower lithosphere.

While the plume/delamination model of Smrekar and Stofan (1997) can predict the large range of topographic corona forms, it does not predict the observed steep relief on some of the troughs which may require a weakness in the lithosphere that allows it to break and be more readily pulled downward (Schubert and Sandwell 1995). In addition, the 800–1000 km diameter of the model corona is much larger than

the average corona diameter of about 253 km (Stofan *et al.* 2001). The plume/delamination model also neglects the effects of a crustal layer. Recent analysis of gravity data suggests that deformation of a crustal layer may play a key role in causing surface topography for coronae (Smrekar and Stofan 2003).

Plume depth

The most successful models of corona formation involve a rising diapir or plume and, more specifically, the later delamination of the lower lithosphere. Where do these plumes originate? Density differences at depth make plume material buoyant and can arise compositionally or thermally. Most diapir models of corona formation neglect the cause of the density difference (Stofan *et al.* 1991, Janes *et al.* 1992, Koch 1994), or assume a thermal contrast (Koch and Manga 1996, Smrekar and Stofan 1997). Hansen (2003) argues that coronae are the result of compositional diapirs, which form as the result of partial melting at relatively shallow depths, possibly heated by a larger plume below. Larger features such as volcanic rises and crustal plateaus are interpreted in this model to be the result of thermal upwellings originating at the core–mantle boundary.

In light of the possible different depths and source mechanisms for upwellings at coronae, Stofan and Smrekar (2005) have proposed an integrated hypothesis of upwelling on Venus, which is based on a model developed for the Earth by Courtillot *et al.* (2003). In this hypothesis the large topographic rises (1000s of kilometres across) are the result of primary plumes from the core–mantle boundary, coronae are suggested to be the result of secondary plumes spawned by the impingement of primary plumes on the upper mantle–lower mantle boundary, and large flow fields and chasmata coronae may result from melting associated with lithospheric extension.

Rayleigh–Taylor lithosphere instability

Tackley and Stevenson (1991) and Tackley *et al.* (1992) were the first to suggest that coronae may form as the result of Rayleigh–Taylor instabilities in the upper mantle. These instabilities may occur when a layer of dense fluid (mantle lithosphere) overlies a layer of less dense fluid (asthenosphere). Small perturbations along the boundary of the fluids can grow until diapirs develop with a characteristic spacing. This method of corona formation has recently been modelled numerically by Hoogenboom and Houseman (2006) using a cylindrical axisymmetric finite element model. The lithosphere is represented by a system of stratified homogeneous viscous layers (low-density crust over high-density mantle, over lower density layer beneath the lithosphere). A small harmonic perturbation imposed on the base of the lithosphere is observed to result in gravitational instability under the constraint of assumed axisymmetry. Topography develops with time under the influence of dynamic stress associated with downwelling or upwelling, and spatially variable crustal thickening or thinning.

Rayleigh–Taylor instability offers an alternative view to the widely accepted plume/delamination model of Smrekar and Stofan (1997). It differs principally in that it does not require a deep thermal plume to initiate and drive the instability, yet it can explain the observational constraints (e.g. topographic profiles, diameter, free-air gravity anomalies). The association of coronae with mantle plumes may be considered open to question, though it may still be the preferred model where voluminous magmatism is observed.

Conclusions

While examination of the basic characteristics of coronae has led many workers to favour mantle upwelling as the origin of coronae, the range in size and morphology of coronae may suggest that not all form by these methods. Modelling involving Rayleigh–Taylor instabilities has shown that the full range of corona profiles can be produced without the need for mantle upwelling and delamination, and has reopened the debate on corona formation mechanisms. The possible heat flow contributed by coronae, and the larger implications for resurfacing and the evolution of Venus as a whole, means that these still relatively poorly understood features are still of great importance for any future studies. The arrival at Venus of the ESA spacecraft Venus Express is expected to advance theories of the venusian atmosphere, but it is clear that there is still much to learn about the surface. Any future mission that could help determine the exact origin of coronae would make a significant contribution to understanding Venus as a whole. ●

Peter M Grindrod, Dept of Earth Sciences, University College London, Gower Street, London, WC1E 6BT, UK; p.grindrod@ucl.ac.uk. Trudi Hoogenboom, Jet Propulsion Laboratory, Pasadena, CA, 91106, USA.

References

Aittola M and V P Kostama 2002 *J. Geophys Res.* **107** 5112 doi:101029/2001JE001528.
Anderson E M 1924 *Dynamics of cone–sheets and ring–dikes* in E B Bailey *et al. Mem. Geol. Surv. Scotland* 11–12.
Anguita F and A F Chiccaro 1991 *Earth, Moon and Planets* 109–116.
Arvidson R E *et al.* 1992 *J. Geophys Res.* **97** 13303–13318.
Barsukov V L *et al.* 1984 *Geochima* **12** 1811–1820.
Barsukov V L *et al.* 1986 *J. Geophys Res.* **91** 378–398.
Basilevsky A T *et al.* 1986 *J. Geophys Res.* **91** 399–411.
Campbell D B and B A Burns 1980 *J. Geophys Res.* **85** 8271–8281.
Copp D L *et al.* 1998 *J. Geophys Res.* **103** 19401–19417.
Courtillot V A *et al.* 2003 *Earth Plan. Sci. Lett.* **205** 295–308.
Glaze L S *et al.* 2002 *J. Geophys Res.* **107** 5135 doi:101029/2002JE001904.
Grindrod P M *et al.* 2005 *J. Geol. Soc. London* **163** 265–275.
Grosfils E B and J W Head 1994 *Geophys Res. Lett.* **21** 701–704.
Hamilton V E and E R Stofan 1996 *Icarus* **121** 171–194.
Hamilton W B 2005 in *Plates, Plumes and Paradigms* ed. G R Foulger *et al. Geol. Soc. Am. Spec. Paper* **388** 781–814.
Hansen V L 2003 *GSA Bull.* **115** 1040–1052.
Hansen V L and R J Phillips 1993 *Science* **260** 526–530.
Hansen V L and R J Phillips 1995 *Geology* **23** 292–296.
Herrick R R 1999 *Geophys Res. Lett.* **26** 803–806.
Herrick R R *et al.* 1997 in *Venus II* eds S W Bougher *et al.* (University of Arizona) 1015–1046.
Herrick R R *et al.* 2005 *J. Geophys. Res.* **110** E01002 doi:101029/2004JE002283.
Hoogenboom T and G A Houseman 2005 *Icarus* **180** 292–307.
Janes D M and S W Squyres 1993 *Geophys. Res. Lett.* **20** 21173–21187.
Janes D M and S W Squyres 1995 *J. Geophys. Res.* **100** 21173–21187.
Janes D M *et al.* 1992 *J. Geophys. Res.* **97** 16055–16067.
Koch D M 1994 *J. Geophys. Res.* **99** 2035–2052.
Koch DM and M Manga 1996 *Geophys. Res. Lett.* **23** 225–228.
Lopez I *et al.* 1999 *Earth, Moon, Plan.* **77** 125–137.
Martin P and E R Stofan 2004 abstract *Lunar Planet. Sci. Conf. XXXV* #1576.
Masursky H 1987 abstract *Lunar Planet. Sci. Conf. XVIII* 598–599.
Masursky H *et al.* 1980 *J. Geophys. Res.* **85** 8232–8260.
McKenzie D *et al.* 1992a *J. Geophys. Res.* **97** 15977–15990.
McKenzie D *et al.* 1992b *J. Geophys. Res.* **97** 13533–13544.
Musser G S and S W Squyres 1997 *J. Geophys. Res.* **102** 6581–6595.
Nikolaeva O N *et al.* 1986 *Geochimia* **5** 279–589.
Price M H *et al.* 1996 *J. Geophys. Res.* **101** 4657–4671.
Pronin A A and E R Stofan 1990 *Icarus* **87** 452–474.
Sandwell D T and G Schubert 1992 *Science* **257** 766.
Schaber G G and J Boyce 1977 in *Impact and Explosion Cratering* (Pergamon Elmsford N Y) 603–612.
Schubert G and D T Sandwell 1995 *Icarus* **117** 173–196.
Schubert G *et al.* 1993 *Icarus* **112** 130–146.
Schultz P H 1976 *Moon* **15** 241–273.
Schultz P H and H Glicken 1979 *J. Geophys Res.* **84** 8033–8047.
Solomon S C *et al.* 1982 *J. Geophys. Res.* **87** 7763–7771.
Smrekar S E and E R Stofan 1997 *Science* **277** 1289–1294.
Smrekar S E and E R Stofan 2003 *J. Geophys. Res.* **108** E8 doi: 101029/2002JE001930.
Squyres S W *et al.* 1992 *J. Geophys. Res.* **97** 13611–13634.
Squyres S W *et al.* 1993 *Geophys. Res. Lett.* **20** 2965–2968.
Stofan E R and J W Head 1990 *Icarus* **83** 216–243.
Stofan E R and S E Smrekar 2005 in *Plates, Plumes and Paradigms* ed. G R Foulger *et al. Geol. Soc. Am. Spec. Paper* **388** 841–861.
Stofan E R *et al.* 1987 abstract *Lunar Planet. Sci. Conf. XVIII* 954–955.
Stofan E R *et al.* 1991 *J. Geophys. Res.* **96** 20933–20946.
Stofan E R *et al.* 1992 *J. Geophys. Res.* **97** 13347–13378.
Stofan E R 1997 in *Venus II: Geology geophysics atmosphere and solar wind environment* ed. S W Bougher *et al.* (Univ. Arizona Press, Tucson) 931–966.
Stofan E R *et al.* 2001 *Geophys. Res. Lett.* **28** 4267–4270.
Tackley P J and D J Stevenson 1991 abstract *Eos Trans. AGU* **72** 287.
Tackley P J *et al.* 1992 abstract in *Papers Presented to the International Colloqium on Venus LPI Contrib* **789** 123–124.
Tapper S W 1997 abstract *Lunar Planet. Sci. Conf. XXVIII* #1415.
Vita–Finzi C *et al.* 2005 in *Plates, Plumes and Paradigms* ed. G R Foulger *et al. Geol. Soc. Am. Spec. Paper* **388** 815–823.
Watters T R and D M Janes 1995 *Geology* **233** 200–204.
Weertman J 1979 *Phys. Earth Planet. Int.* **19** 197–207.